Princeton Plasma Physics Laboratory

PPPL- 4394

PPPL- 4394

A Spatially Resolving X-ray Crystal Spectrometer for Measurement of Ion-temperature and Rotation-velocity Profiles on the Alcator C-Mod Tokamak

K.W. Hill, M. L. Bitter, S.D. Scott, A. Ince-Cushman, M. Reinke, J.E. Rice,
P. Beiersdorfer, M.-F. Gu, S.G. Lee, Ch. Broennimann, and E.F. Eikenberry

March, 2009

PPPL
PRINCETON PLASMA
PHYSICS LABORATORY

Prepared for the U.S. Department of Energy under Contract DE-AC02-76CH03073.

Princeton Plasma Physics Laboratory
Report Disclaimers

Full Legal Disclaimer

Trademark Disclaimer

PPPL Report Availability

Princeton Plasma Physics Laboratory:

http://www.pppl.gov/techreports.cfm

Office of Scientific and Technical Information (OSTI):

http://www.osti.gov/bridge

Related Links:

U.S. Department of Energy

Office of Scientific and Technical Information

Fusion Links

A spatially resolving x-ray crystal spectrometer for measurement of ion-temperature and rotation-velocity profiles on the Alcator C-Mod tokamak[a…]

K. W. Hill,[1] M. L. Bitter,[1] S. D. Scott,[1] A. Ince-Cushman,[2] M. Reinke,[2] J. E. Rice,[2] P. Beiersdorfer,[3] M.-F. Gu,[3] S. G. Lee,[4] Ch. Broennimann,[5] and E. F. Eikenberry[5]
[1]*PPPL, Princeton University, P.O. Box 451, Princeton, New Jersey 08543, USA*
[2]*PSFC, MIT, Cambridge, Massachusetts 02139, USA*
[3]*LLNL, Livermore, California 94550, USA*
[4]*National Fusion Research Institute, Taejeon 305-333, South Korea*
[5]*DECTRIS Ltd., CH-5232 Villigen-PSI, Switzerland*

(Presented 12 May 2008; received 12 May 2008; accepted 17 July 2008; published online 31 October 2008)

A new spatially resolving x-ray crystal spectrometer capable of measuring continuous spatial profiles of high resolution spectra ($\lambda/d\lambda > 6000$) of He-like and H-like Ar $K\alpha$ lines with good spatial (~1 cm) and temporal (~10 ms) resolutions has been installed on the Alcator *C*-Mod tokamak. Two spherically bent crystals image the spectra onto four two-dimensional Pilatus II pixel detectors. Tomographic inversion enables inference of local line emissivity, ion temperature (T_i), and toroidal plasma rotation velocity (v_ϕ) from the line Doppler widths and shifts. The data analysis techniques, T_i and v_ϕ profiles, analysis of fusion-neutron background, and predictions of performance on other tokamaks, including ITER, will be presented. © *2008 American Institute of Physics*. [DOI: 10.1063/1.2969080]

I. INTRODUCTION

Understanding thermal transport in plasmas is an important topic in magnetic fusion energy (MFE) research. Theoretical simulations of ion thermal transport based on, e.g., ion-temperature gradient (ITG) modes require good measurements of the ion-temperature (T_i) profile and its gradient. The plasma rotation velocity (v_ϕ) and its gradients can also profoundly affect thermal transport and confinement. In reactors, the rotation profile will not likely be determined by neutral beam injection (NBI) but by self-generated mechanisms; thus, it is important to understand the physics of intrinsic rotation. In this paper we report on a new diagnostic, the imaging x-ray crystal spectrometer[1,2] (XCS), which uses spatially resolved high resolution spectroscopy of highly ionized impurities in the Alcator *C*-Mod tokamak at MIT, in order to measure local T_i and v_ϕ from the Doppler broadening and Doppler shifts of a spectral line. Unlike charge-exchange-recombination-spectroscopy (CXRS) techniques, the imaging XCS does not require either a heating or a diagnostic neutral beam. The new features of the instrument are as follows: (1) the use of a spherically bent x-ray diffracting crystal to both (a) disperse the spectrum in one plane via the Bragg relation

$$n\lambda = 2d \sin\theta \tag{1}$$

and (b) image the spectra in a perpendicular plane via the astigmatism of the spherically bent reflector; (2) the use of a new, high count-rate, pixilated two-dimensional (2D) imaging x-ray detector[3] to record the spatially resolved spectra; (3) the use of tomographic inversion techniques[4] to infer local plasma parameters from many chordally integrated spectra; and (4) the replacement of multiple single-chord spectrometers by a single instrument, which is simple in concept and implementation and provides data of much higher quality and usefulness. In Eq. (1), λ is the x-ray wavelength, d is the lattice spacing of the crystal, n is the order of diffraction, and θ is the Bragg angle or angle between the incident x-ray direction and the surface of the crystal.

II. DESCRIPTION OF SPECTROMETER

The principle of the spatially resolving or imaging XCS has been described in detail by others[1,2] and will be only briefly reviewed here. A drawing that illustrates the principle and the main components of the imaging XCS recently installed on Alcator *C*-Mod is shown in Fig. 1. He-like and H-like Ar $K\alpha$ x rays from the plasma to the right of "B-port" pass through the gray adaptor section, the gate valve, and a 0.001 in. thick Be vacuum window, impinge onto the two spherically bent crystals labeled "He-like" and "H-like," and are diffracted to their respective detectors. Both crystals are quartz with a 2D spacing of 4.562 Å and radii of curvature of 1.4 and 1.5 m. One crystal is rectangular with dimensions of 3.8×6.4 cm^2, and the other is circular with a diameter of 6 cm. The distance from the crystals to the plasma is about 3.0 m. In operation, the crystals and detectors are contained inside a closed, Al box containing 1 atm of He to avoid the attenuation of x rays, which would occur in air. The locus of x-ray beams of fixed λ or Bragg angle which diffract from a

[a]Contributed paper, published as part of the Proceedings of the 17th Topical Conference on High-Temperature Plasma Diagnostics, Albuquerque, New Mexico, May 2008.

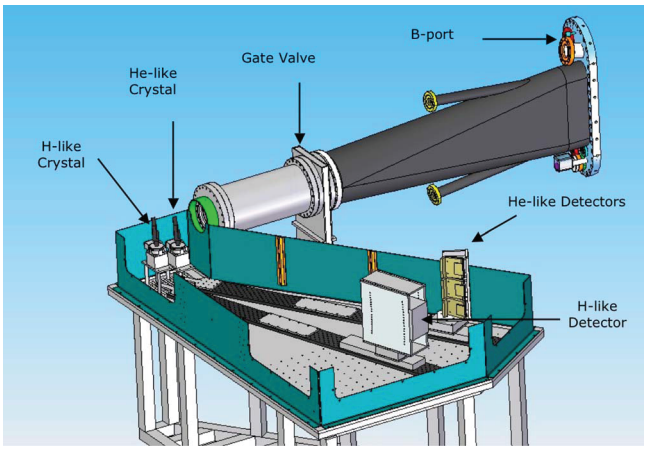

FIG. 1. (Color online) Schematic of the imaging spectrometer which was installed on Alcator *C*-Mod in April 2007.

point on the crystal defines two cones, one from the plasma and incident onto the crystal and the other from the crystal to the 2D detector. Thus, the conical section of x rays from the plasma diffracts from the crystal and forms a conical-section image on the detector, preserving the vertical spatial order of the plasma x-ray image.

The good time resolution of the imaging XCS is enabled by the high photon flux onto the detectors, which is typically 5–10 MHz in the He-like Ar resonance line, *w*, for a central chord with ~1 cm spatial resolution; single-chord count rates as high as 40 MHz have been recorded. The detectors are Pilatus II pixilated silicon detectors with 195×487 square pixels of 0.172 mm on a side. Each pixel has its own amplifier, threshold, and counting electronics and 20 bit storage register and can count at rates up to 1 MHz.

The H-like Ar spectrometer was installed as a check on the tomographic inversion of the He-like Ar spectra, which can become quite hollow at high electron temperatures ($T_e > 3$ keV). Thus, the chord-integrated He-like Ar spectra sample cooler, noncentral regions of the plasma, whereas the H-like argon should remain peaked at much higher temperatures and should more accurately reflect the maximum temperature along the chord.

III. DATA ANALYSIS TECHNIQUE

Three Pilatus II detectors, each with 195 columns of pixels in the spectral direction and 487 rows of pixels in the vertical, imaging dimension, are used to record the spectra from the full height of the Alcator *C*-Mod plasma. In the PPPL analysis technique, the 1461 rows of spectral data are typically grouped into 48 equally spaced chordal views, which are summed to improve statistics. This grouping provides a vertical spatial resolution of about 1.3 cm at the plasma center, or a radial spatial resolution of about 0.9 cm for a typical plasma elongation of 1.5. Prior to vertically binning the pixels, however, the inherent curvature of the spectral lines on the detector is removed by a linear reapportionment of the counts in neighboring pixels. The line curvature is defined by the ellipse resulting from the intersection of the diffracting cone,

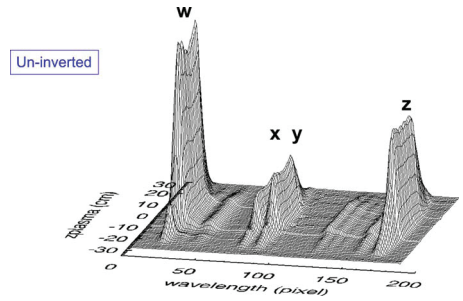

FIG. 2. (Color online) He-like Ar spectra as a function of plasma height for ~45 chord analysis of imaging XCS data.

$$\theta = \arcsin(2d/n\lambda), \tag{2}$$

from a point on the crystal with the detector plane. Any remaining curvature of the spectral line due to a nonconstant velocity profile is small compared to the elliptical curvature and should contribute negligibly to the line width or shift for a particular chord, thus validating the vertical binning of ~30 rows of pixels per chord. The data are typically collected every 20 ms, but in some cases, a 5 ms timing has been utilized.

Typical high resolution spectra of He-like Ar lines after removal of curvature as a function of vertical position *z* in the plasma are shown in Fig. 2.

Following removal of the curvature, a Gaussian function plus a linear background is fitted to regions around selected spectral lines, such as lines *w* and *z*. Relative line brightness is inferred from the area of the Gaussian, T_i is inferred from the line width, and a component of v_ϕ is inferred from the centroid shift. Relative spectral calibration for the non-Doppler-shifted positions of the lines are inferred in locked mode discharges in which the plasma rotation is small or nonexistent. Local values of line emissivity T_i and v_ϕ are determined by applying a tomographic inversion algorithm.[4]

IV. ION-TEMPERATURE AND ROTATION-VELOCITY MEASUREMENTS

The imaging XCS provides data for T_i and v_ϕ determination with very good temporal (~10–20 ms) and spatial (~1 cm) resolutions. The resulting T_i and v_ϕ profiles inferred from the noninverted or chordally integrated He-like Ar resonance line *w* are shown as a function of the vertical position in the plasma core and time in Figs. 3 and 4 for a H-mode discharge with 3 MW of ion cyclotron range of frequencies (ICRF) heating. The T_i profile in Fig. 3 is narrow near the beginning of the discharge with a maximum value

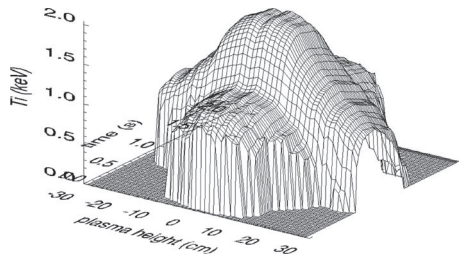

FIG. 3. Ion-temperature profiles vs time inferred from noninverted He-like Ar spectra.

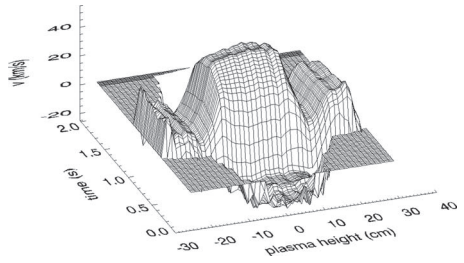

FIG. 4. Rotation-velocity profiles vs time in an ICRF heated H-mode discharge, inferred from noninverted spectra.

near 1.0 keV. After the ICRF turns on near 0.6 s, the central value of T_i increases to about 2.0 keV, and the profile broadens substantially. Prior to ICRF heating in Fig. 4, the rotation velocity is ~ -15 km/s. After ICRF heating is applied and the plasma makes a transition to the H mode, the central rotation velocity increases to ~ 40 km/s in the core.

A confirmation of the validity of the tomographic inversion of the He-like Ar spectra is indicated by Figs. 5 and 6. Figure 5 illustrates "noninverted" T_i versus plasma height z a few times in a discharge inferred from Gaussian fits to the chord-integrated spectra (noninverted) of both He-like Ar and H-like Ar. Note that near a time of 1 s in the discharge, the He-like spectra indicate an apparent T_i near 2 keV, whereas the inference from the H-like spectra is closer to 2.5 keV. However, the local central T_i value inferred from the inverted spectra in Fig. 6(a) is about 2.5 keV, in agreement with the measurement from the centrally peaked H-like spectra in Fig. 5, thus instilling confidence in the inversion process for the very hollow He-like Ar density, as shown in Fig. 6(b).

Another check on the accuracy of the imaging XCS T_i profile measurements is shown in Fig. 7, which compares the XCS T_i measurements from the inverted He-like Ar spectra with other T_i and electron temperature (T_e) measurements at a time when the electron density was about 3×10^{20} m^{-3} and, thus, T_i and T_e should be about equal. We see that the XCS T_i measurement agrees with the central value of T_i inferred from the neutron flux, extrapolates to the T_i measurements in the edge from the CXRS diagnostic, and is in

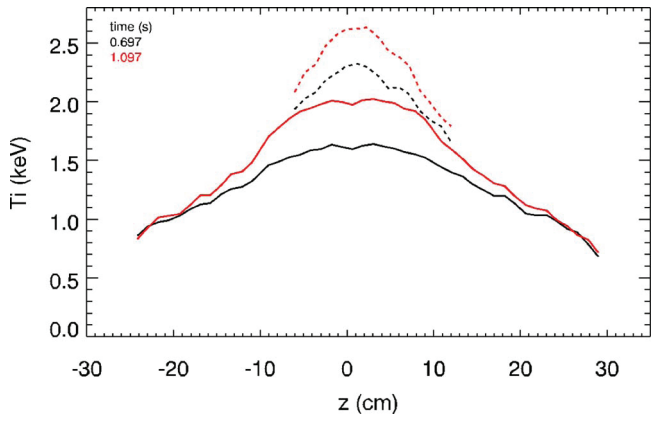

FIG. 5. (Color online) Comparison of T_i profiles three times inferred from noninverted He-like (solid) and H-like (dashed) Ar spectra.

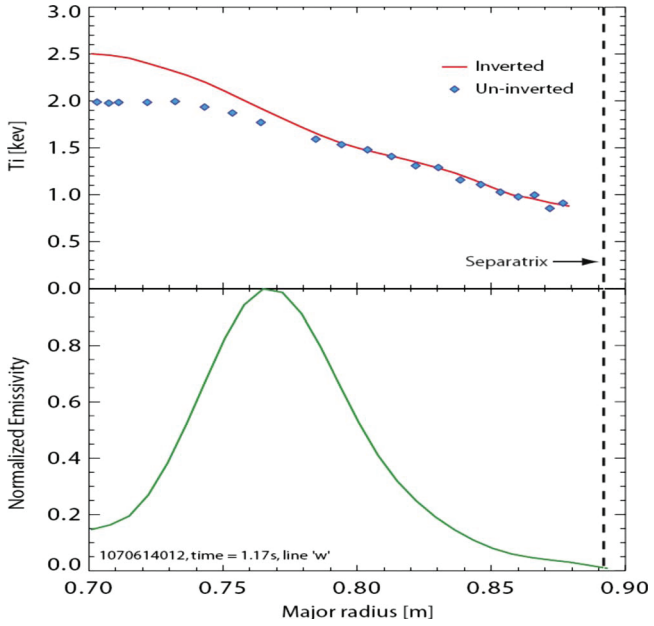

FIG. 6. (Color online) (a) T_i inferred from inverted (solid) and noninverted He-like Ar spectra. (b) Calculated density of He-like Ar.

reasonable agreement with T_e measurements from the Thomson scattering (TS) and grating polychromator electron-cyclotron emission diagnostics.

V. DISCUSSION

The spatially resolving XCS has been routinely in use to provide T_i and v_ϕ measurements from almost all *C*-Mod plasmas since its installation in April 2007 and is contributing to the *C*-Mod physics program. This instrument has also been selected for use on the international tokamak, ITER, and responsibility for building the ITER XCS has been assigned jointly to the U.S. and India. Considerable design work, intensity calculations, and neutronics calculations for the ITER XCS have been done, and application of the instrument to ITER looks favorable.[5]

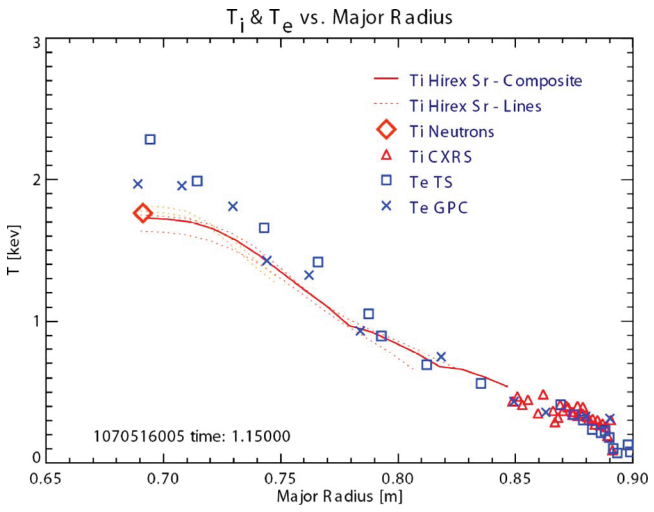

FIG. 7. (Color online) T_i profile from imaging XCS He-like Ar spectra (solid) agrees with neutron and CXRS T_i measurements and with T_e from TS and the grating polychromator (GPC) as expected at high densities ($n_e \sim 3\times10^{20}$ m^{-3}).

Scaling of the temporal resolution obtained on *C*-Mod to larger, lower density tokamaks having similar impurity concentration and n_e profile shapes and the same number of chords is reasonably favorable since the count rate per chord scales as $a^2 n_e^2$,[6] where a is the minor radius, and the plasma is assumed to be of the same distance from the crystal for both tokamaks. The n_e^2 term describes the scaling of volume emissivity, one factor of a accounts for the surface-brightness scaling due to the path-length integral, and the second factor of a results from the vertical height of the surface subtended by the viewing chord. Thus, for the above assumptions, e.g., NSTX, having $a=0.68$ m and operating at a central density $n_{e0}=7.7\times10^{19}$ m^{-3}, would produce the same count rate per chord as *C*-Mod with $n_{e0}=2.5\times10^{20}$ m^{-3} and $a=0.21$ m.

The imaging XCS with Pilatus II detector has a high tolerance to background counts due to fusion neutrons and gamma rays, which is favorable for adapting the diagnostic to NBI heated tokamaks and to, e.g., ITER. The high tolerance results from (a) a small pixel surface area, (b) a low counting efficiency for the 0.03 cm thick detector, ~0.003, for energetic neutrons, and (c) the ~1 MHz count-rate capability of the individual pixel electronics. The per pixel background count rate in an unshielded Pilatus detector in the *C*-Mod test cell was about 20 counts/s pixel for a total *C*-Mod neutron production rate of about 6×10^{13} n/s. This neutron/gamma-ray induced background could be reduced by a factor of >50 by surrounding the detector, except for an x-ray entrance tunnel, with shielding. For comparison, the per pixel count rate due to x rays in the peak of the He-like Ar spectral line *w* from a central chord is typically 10 000 counts/s pixel, and count rates as high as 200 000 counts/s pixel have been observed. Count rates in chords further from the core are one to two orders of magnitude lower. Also, the Pilatus II detector was built using radiation hardening technology and has been tested to a fluence of 10^{14} 1 MeV neutrons/cm^2. Neutronics simulations[5] indicate that a properly shielded Pilatus II detector installed near the back of an ITER port plug can survive the expected 10^7 s lifetime of ITER operation.

ACKNOWLEDGMENTS

This work was supported by the U.S. Department of Energy Contract Nos. DE-AC02-76CHO3073 and DE-FC02-99ER54572.

[1] M. Bitter, K. W. Hill, B. Stratton, A. L. Roquemore, D. Mastrovito, S. G. Lee, J. G. Bak, M. K. Moon, U. W. Nam, G. Smith *et al.*, Rev. Sci. Instrum. **75**, 3660 (2004).
[2] A. Ince-Cushman, J. E. Rice, M. Bitter, M. L. Reinke, K. W. Hill, M. F. Gu, E. Elkenberry, C. Broennimann, S. Scott, Y. Podpaly *et al.*, Rev. Sci. Instrum. **79**, 10E302 (2008).
[3] See http://pilatus.web.psi.ch/pilatus.htm for a description of the Pilatus II detector.
[4] I. Condrea, E. Haddad, B. C. Gregory, and G. Abel, Phys. Plasmas **7**, 3641 (2000).
[5] S. Davis, R. Barnsley, and R. Pampin, "ITER x-ray crystal spectroscopy," UKAEA Report No. EFDA05-1350 D5.1.
[6] R. Bartiromo, R. Giannella, M. L. Apicella, F. Bombarda, S. Mantovani, and G. Pizzicaroli, Nucl. Instrum. Methods Phys. Res. A **225**, 378 (1984).

The Princeton Plasma Physics Laboratory is operated
by Princeton University under contract
with the U.S. Department of Energy.

Information Services
Princeton Plasma Physics Laboratory
P.O. Box 451
Princeton, NJ 08543

Phone: 609-243-2750
Fax: 609-243-2751
e-mail: pppl_info@pppl.gov
Internet Address: http://www.pppl.gov